HHS Public Access

Author manuscript

Am J Med Genet A. Author manuscript; available in PMC 2019 February 01.

Published in final edited form as:

Am J Med Genet A. 2018 February ; 176(2): 386–390. doi:10.1002/ajmg.a.38563.

Spontaneously regressing brain lesions in Smith-Lemli-Opitz syndrome

An N. Dang Do[#1,*], **Eva H. Baker**[#2], **Katherine E. Warren**[3], **Simona E. Bianconi**[1], and **Forbes D. Porter**[1]

[1]Division of Translational Research, *Eunice Kennedy Shriver* National Institute of Child Health and Human Development (NICHD), National Institutes of Health, Bethesda, MD

[2]Department of Radiology and Imaging Sciences, Clinical Center, National Institutes of Health, Bethesda, MD

[3]Center for Cancer Research, National Cancer Institute, National Institutes of Health, Bethesda, MD

[#] These authors contributed equally to this work.

Abstract

Smith-Lemli-Opitz syndrome (SLOS) is a metabolic disorder caused by an inborn error of cholesterol synthesis that affects the development of many organ systems. Malformations in the central nervous system typically involve midline structures and reflect abnormal growth and differentiation of neurons and supporting cells. Despite these defects in central nervous system development, brain tumor formation has only rarely been reported in association with SLOS. We present three individuals with SLOS and lesions in the basal ganglia or brainstem detected by MRI that were concerning for tumor formation. However, the individuals' clinical and neurological course remained stable, and the lesions regressed after several years. These lesions have similarities to spongiotic changes observed in individuals with neurofibromatosis type 1 (NF1). Notably, impaired activity of small GTPases is present in both SLOS and NF1, perhaps giving mechanistic insight into the formation of these lesions.

Keywords

regressing brain lesions; spongiotic changes; GTPases; Smith-Lemli-Opitz syndrome; neurofibromatosis type 1

INTRODUCTION

Smith-Lemli-Opitz syndrome (SLOS) is a neurodevelopmental disorder of cholesterol synthesis, secondary to reduced activity of the enzyme sterol delta-7-dehydrocholesterol reductase (DHCR7). The classical SLOS phenotype involves craniofacial dysmorphisms, developmental and growth delays, behavioral disturbances, and 2–3 toe syndactyly. A

[*]Corresponding Author: An N. Dang Do, 10 Center Drive, Room 2-5132, Bethesda, MD 20892, Phone: 301.496.8849, Fax: 301.402.0574, an.dangdo@nih.gov.

scoring system for evaluating the severity of SLOS presentation organizes the key features into ten organ systems, distinguished by their embryological origin [Bialer *et al.* 1987; Kelley and Hennekam 2000]. Findings generating a score in the brain category include "major CNS malformations, gyral defects, qualitative MRI abnormality, and seizures" [Kelley and Hennekam 2000]. A retrospective review of brain imaging studies in 55 individuals with SLOS revealed that the most common brain abnormalities involve midline and para-midline structures [Lee *et al.* 2013]. The authors introduced a brain severity score based on these findings. Other reviews of brain tissues from individuals with SLOS revealed poor development of the corpus callosum, disordered arrangements of cellular layers in the cerebellum, and abnormal development of cerebral gyri [Cherstvoy *et al.* 1984; Curry *et al.* 1987]. Malignant brain lesions in individuals with SLOS have been reported in two cases [Oslejskova *et al.* 2008; Aslan *et al.* 2017].

In this report, we describe brain lesions detected by MRI in 3 individuals with SLOS. The lesions had benign imaging features and no clinical symptoms specifically attributable to the lesions were identified. Thus, the lesions were followed to resolution, without biopsy or treatment. Some of the imaging features, and, in particular, the temporal pattern, are similar to the spongiform myelopathy found in neurofibromatosis type 1 (NF1). We speculate that dysregulation of small GTPases activity may play a role in the development of these apparently benign brain lesions in individuals with SLOS.

MATERIALS AND METHODS

The individuals presented here were enrolled in a natural history study approved by the *Eunice Kennedy Shriver* NICHD IRB in Bethesda, Maryland (NCT00001721). Informed, written consent was obtained from guardians. Brain MRI performed as part of this protocol used a 1.5T GE (1999–2010) and a 3T Philips scanner. The exams initially included T1-weighted, proton-density weighted, and T2-weighted images. Later studies were performed with higher resolution and omitted the proton-density weighted, but added FLAIR, diffusion tensor imaging (DTI), and susceptibility-weighted images. Post-contrast T1-weighted images, MR perfusion imaging, MR spectroscopy, head CT, and FDG-PET scans were acquired for some patients. Clinical and medication details of the 3 individuals are provided in Supplemental Table 1.

PATIENTS

Individual 1 was a Caucasian male born at 39 weeks estimated gestational age to a 39-year-old G12P0 mother. Weight and length at birth were 3991 g (85th centile), and 56 cm (>97th centile). Early development was notable for poor feeding and weight gain. At 2 years, he had delayed speech and language development, and impulsive behavior. He walked independently at 19 months, and spoke 2–3 words sentences at 4 years. He developed seizure-like activity at 7 years without any abnormal findings on electroencephalogram. SLOS was diagnosed and he was enrolled in the study at age 9 years. His exam at study entry showed intact function of cranial nerves 2–12, and lower than average muscle bulk and tone. A developmental assessment at age 23 years showed a Stanford Binet score of 66 (mean 100, standard deviation 15).

At age 9 years, brain MRI revealed a discrete 4-mm lesion spanning the boundary between the tail of the left putamen and the most posterior part of the globus pallidus. Follow-up exams at age 9 years 7 months and 10 years 3 months revealed slight growth of the lesion (4.5 mm and 5.5 mm, respectively). The signal characteristics of this lesion are as described in Figure 1. The patient refused to have follow-up MRI exams until 23 years 3 months, when the exam revealed no evidence of a lesion at that location. The patient also had several stable minor structural anomalies (Supplemental Table 1). His neurological function and exam were unchanged from baseline throughout this period. No seizures occurred after age 12 years.

Individual 2 was a Caucasian male born at term to a 30-year-old G2P1 mother. Weight and length at birth were 3260 g (25th centile), and 54 cm (90th centile). Head circumference was 33.5 cm (10th centile). He had a history of failure to thrive with oral aversions. He had an older brother and a paternal first cousin with SLOS. SLOS was diagnosed at age 22 months, and he enrolled in the study at age 33 months. His exam at study entry showed mild developmental delay, and intact function of cranial nerves 2–12. He developed selective mutism beginning at age 3 years. Developmental assessments at ages 9 and 16 years showed Stanford Binet scores of 65 and 70, respectively. He had no seizures.

His first brain MRI at age 3 years 3 months revealed several minor structural anomalies (Supplemental Table 1), but no visible discrete lesion. Follow-up brain MRI at age 4 years 5 months demonstrated a 4-mm lesion in the pons near the anterior margin and slightly left of midline. At age 5 years 10 months, the lesion had enlarged to 12 mm, crossing the midline and protruding into the pre-pontine cistern. At age 7 years 7 months, the lesion further protruded into the pre-pontine cistern and enlarged to 16 mm, its largest measured size. At age 16 years 9 months, the lesion was no longer visible, but there was slight residual expansion of the left anterior pons. The signal characteristics of this lesion are as described in Figure 1. The evolution of this lesion is shown in Figure 2. His neurological function and exam remained unchanged throughout.

Individual 3 was a Caucasian male born at 41 weeks estimated gestational age to a G3P1 mother. Birth weight was 3501 g (50th centile). He had feeding problems and hypotonia from birth. Autism was diagnosed around age 3 years and SLOS 5 months later. His exam at study entry at age 7 years 5 months revealed hypotonia, and limited social interaction on exam. He had no focal neurological deficits, and no history of seizures. Developmental assessments at ages 5 and 11 years showed Mullen scores of 35 and 36, respectively.

An outside MRI scan at 3 years 10 months revealed minor structural anomalies (Supplemental Table 1), but no visible intraparenchymal lesion. Initial imaging at study enrollment showed a nearly round, 5.5 mm lesion in the right globus pallidus. The lesion slightly expanded the margins of the globus pallidus on 3D T1-weighted images. Multiple follow-up MRI exams were obtained that demonstrated gradual slight enlargement of the lesion; the maximum lesion size was 7 mm at age 10 years 4 months. The most recent lesion size was 4 mm at age 12 years 4 months. We intend to continue following this lesion until it resolves. A selection of this individual’s images is presented in Figure 1.

DISCUSSION

The individuals presented here have confirmed diagnoses of SLOS based on clinical, biochemical, and molecular findings. Macroscopically on MRI, the lesions were not present in early childhood (Individuals 2, 3), and resolved over time (Individuals 1, 2). In all 3 cases the lesions had MRI characteristics that favored non-malignancy: small with well-circumscribed margins, no edema, no enhancement with contrast material, and very slow growth. Attributable symptoms were not present. The lesions were in locations difficult to biopsy, therefore close observation was preferred. The resolution of the lesions in two of the individuals, and regression in the third confirm the benign and spontaneously-regressing nature of the lesions. The prevalence of tumor-like brain lesions in our cohort of individuals with SLOS who underwent brain imaging is unusually high (3 in 55) compared to the reported rate of incidental brain neoplasms discovered in normal volunteers (2–3 in 1000) [Katzman *et al.* 1999], suggesting a non-random association.

Brain malignancy in individuals with SLOS has been reported in two cases [Oslejskova *et al.* 2008; Aslan *et al.* 2016], although biochemical or molecular confirmation for the diagnosis of SLOS was not provided in the latter reference. Both groups suggested dysregulation of the Shh signaling pathway to be the potential underlying tumorigenesis mechanism. This hypothesis is not congruent with current findings of downregulated Shh signaling in SLOS [Cooper *et al.* 2003], as compared to upregulated Shh signaling in the development of gliomas and medulloblastomas [Guizzetti and Costa 2008; Traiffort *et al.* 2010].

The MRI characteristics of the lesions we report have multiple similarities to the spontaneously regressing lesions seen in NF1, variously termed vacuolar myelinopathy, spongiform gliosis, or unidentified bright objects (UBOs). Spongiform gliosis is found in more than half of individuals with NF1 [Van Es *et al.* 1996]. Histopathology of brain lesion tissue from deceased patients with NF1 showed intramyelinic spongiotic or vacuolar changes [DiPaolo *et al.* 1995]. In measuring water T2 and diffusivity within the lesions, Billiet *et al.* [2014] concluded that altered microstructural compartmentalization led to an increase in “extracellular-like” intracellular water, consistent with the vacuoles between myelin layers in intramyelinic edema. The evolution of NF1 and SLOS lesions follows a similar time course: both appear spontaneously early in childhood, grow slowly, and then regress as the patient enters the teenage years. NF1 UBOs have been described to decrease in frequency as the age of the affected populations increased [Gill *et al.* 2006]. Similarly, Payne *et al.* [2014] observed that almost half of the discrete T2 hyperintense lesions completely resolved, while 14% became diffuse. Lesions in the basal ganglia, brainstem, and thalamus were most likely to resolve [Gill *et al.* 2006; Payne *et al.* 2014]. Contrasting with the NF1 UBOs, the lesions reported here were solitary rather than multiple [Van Es *et al.* 1996]. In addition, the pons (the location of the lesion in Individual 3) is an uncommon site for NF1 UBOs.

Neurofibromin, the protein affected in NF1, has Ras GTPase activating function that enables it to suppress growth signaling through the Ras-MAPK pathway. Loss of neurofibromin expression is hypothesized to underlie the uncontrolled growth of Schwann cells and the development of neurofibromas seen in NF1 [Arun and Gutmann 2004]. Whether

dysregulation of these small GTPases and their downstream pathways results in the lesions seen on brain imaging remains undetermined. Interestingly, UBOs on brain MRI have also been reported in 4 of 30 individuals actively using amphetamine [Fatovich *et al*. 2010]. In addition, Wheeler *et al*. [2015] showed that amphetamine activated Rho and Rac GTPases, leading downstream effect on extracellular dopamine availability.

Several cellular pathways have been implicated in neuronal malformations in SLOS. Decreased cholesterol and other sterols have been linked to down regulation of the Sonic hedgehog (Shh) signaling *cascade in* vitro and in animal models [Cooper *et al*. 2003; Sever *et al*. 2016]. Separately, Francis *et al*. [2016] observed that the accumulation of 7-DHC in iPSCs inhibited protein complex formation in the Wnt/β-catenin pathway. Work in an SLOS mouse model has shown that increased phosphorylation of upstream Rho GTPase complexes was associated with abnormal development of neuronal processes [Jiang *et al*. 2010]. Defective Rho GTPases activity has been associated with other human disorders of mental development [von Bohlen Und Halbach 2010].

From a mechanistic standpoint, both SLOS and NF1 have disordered regulation of signaling pathways involving small GTPases. In NF1, upregulation of Ras GTPase/Rho GTPase activity promotes growth of Schwann cells [Harrisingh and Lloyd 2004]. In SLOS, although altered Ras signaling was not observed, Jiang *et al*. [2010] demonstrated increased activation of Rho/Rac GTPases in brain tissue from *Dhcr7* mutant mice. We speculate a common mechanism for these similar brain lesions in NF1 and SLOS.

Supplementary Material

Refer to Web version on PubMed Central for supplementary material.

ACKNOWLEDGMENTS

We thank the patients and their families for their participation. We also thank Audrey Thurm, PhD and Cristan Farmer who provided the developmental assessment scores; and the MRI and PET technologists who acquired the images of these patients: Jeanette Black, Mary Busse, Kimberly Chung, Bonita Damaska, Sandra Hess, Renee Hill, Michael Kreigh, Sandra McKee, Mastaneh Owhadi, James Sedlacko, Theresa Tyler, Ronald White, Victor Wright, and Sema Yessaian. ADD, SB, and FDP are supported by the Intramural Research Program of the *Eunice Kennedy Shriver* NICHD. The authors have no conflict of interest to declare.

REFERENCES

Arun D, Gutmann DH. 2004 Recent advances in neurofibromatosis type 1. Current opinion in neurology 17(2):101–105. [PubMed: 15021234]

Aslan A, Borcek AO, Pamukcuoglu S, Baykaner MK. 2017 Intracranial undifferentiated malign neuroglial tumor in Smith-Lemli-Opitz syndrome: A theory of a possible predisposing factor for primary brain tumors via a case report. Child's nervous system 33(1):171–177.

Bialer MG, Penchaszadeh VB, Kahn E, Libes R, Krigsman G, Lesser ML. 1987 Female external genitalia and mullerian duct derivatives in a 46,XY infant with the smith-lemli-Opitz syndrome. American journal of medical genetics 28(3):723–731. [PubMed: 3322011]

Billiet T, Madler B, D'Arco F, Peeters R, Deprez S, Plasschaert E, Leemans A, Zhang H, den Bergh BV, Vandenbulcke M, Legius E, Sunaert S, Emsell L. 2014 Characterizing the microstructural basis of "unidentified bright objects" in neurofibromatosis type 1: A combined in vivo multicomponent T2 relaxation and multi-shell diffusion MRI analysis. NeuroImage Clinical 4:649–658. [PubMed: 24936416]

Cherstvoy ED, Lazjuk GI, Ostrovskaya TI, Shved IA, Kravtzova GI, Lurie IW, Gerasimovich AI. 1984 The Smith-Lemli-Opitz syndrome. A detailed pathological study as a clue to a etiological heterogeneity. Virchows Archiv A, Pathological anatomy and histopathology 404(4):413–425. [PubMed: 6437074]

Cooper MK, Wassif CA, Krakowiak PA, Taipale J, Gong R, Kelley RI, Porter FD, Beachy PA. 2003 A defective response to Hedgehog signaling in disorders of cholesterol biosynthesis. Nature genetics 33(4):508–513. [PubMed: 12652302]

Curry CJ, Carey JC, Holland JS, Chopra D, Fineman R, Golabi M, Sherman S, Pagon RA, Allanson J, Shulman S, et al. 1987 Smith-Lemli-Opitz syndrome-type II: multiple congenital anomalies with male pseudohermaphroditism and frequent early lethality. American journal of medical genetics 26(1):45–57. [PubMed: 3812577]

DiPaolo DP, Zimmerman RA, Rorke LB, Zackai EH, Bilaniuk LT, Yachnis AT. 1995 Neurofibromatosis type 1: pathologic substrate of high-signal-intensity foci in the brain. Radiology 195(3):721–724. [PubMed: 7754001]

Fatovich DM, McCoubrie DL, Song SJ, Rosen DM, Lawn ND, Daly FF. 2010 Brain abnormalities detected on magnetic resonance imaging of amphetamine users presenting to an emergency department: a pilot study. The medical journal of Australia 193(5):266–268. [PubMed: 20819043]

Francis KR, Ton AN, Xin Y, O'Halloran PE, Wassif CA, Malik N, Williams IM, Cluzeau CV, Trivedi NS, Pavan WJ, Cho W, Westphal H, Porter FD. 2016 Modeling Smith-Lemli-Opitz syndrome with induced pluripotent stem cells reveals a causal role for Wnt/beta-catenin defects in neuronal cholesterol synthesis phenotypes. Nature medicine 22(4):388–396.

Gill DS, Hyman SL, Steinberg A, North KN. 2006 Age-related findings on MRI in neurofibromatosis type 1. Pediatric radiology 36(10):1048–1056. [PubMed: 16912896]

Guizzetti M, Costa LG. 2008 Sonic hedgehog in Smith-Lemli-Opitz syndrome and tumor development. Journal of pediatric hematology/oncology 30(9):641–642. [PubMed: 18776754]

Harrisingh MC, Lloyd AC. 2004 Ras/Raf/ERK signalling and NF1. Cell cycle (Georgetown, Tex) 3(10):1255–1258.

Jiang XS, Wassif CA, Backlund PS, Song L, Holtzclaw LA, Li Z, Yergey AL, Porter FD. 2010 Activation of Rho GTPases in Smith-Lemli-Opitz syndrome: pathophysiological and clinical implications. Human molecular genetics 19(7):1347–1357. [PubMed: 20067919]

Katzman GL, Dagher AP, Patronas NJ. 1999 Incidental findings on brain magnetic resonance imaging from 1000 asymptomatic volunteers. JAMA 282(1):36–39. [PubMed: 10404909]

Kelley RI, Hennekam RC. 2000 The Smith-Lemli-Opitz syndrome. Journal of medical genetics 37(5): 321–335. [PubMed: 10807690]

Lee RW, Conley SK, Gropman A, Porter FD, Baker EH. 2013 Brain magnetic resonance imaging findings in Smith-Lemli-Opitz syndrome. American journal of medical genetics Part A 161A(10): 2407–2419. [PubMed: 23918729]

Nowaczyk MJ, Irons MB. 2012 Smith-Lemli-Opitz syndrome: phenotype, natural history, and epidemiology. Am J Med Genet C Semin Med Genet 160C(4):250–262. [PubMed: 23059950]

Oslejskova H, Horinova V, Sterba J, Pavelka Z, Babovic-Vuksanovic D, Dubska L, Valik D. 2008 Malignant intracranial germinoma in Smith-Lemli-Opitz syndrome: cholesterol homeostasis possibly connecting morphogenesis and cancer development. Journal of pediatric hematology/ oncology 30(9):689–691. [PubMed: 18776762]

Payne JM, Pickering T, Porter M, Oates EC, Walia N, Prelog K, North KN. 2014 Longitudinal assessment of cognition and T2-hyperintensities in NF1: an 18-year study. American journal of medical genetics Part A 164A(3):661–665. [PubMed: 24357578]

Sever N, Mann RK, Xu L, Snell WJ, Hernandez-Lara CI, Porter NA, Beachy PA. 2016 Endogenous B-ring oxysterols inhibit the Hedgehog component Smoothened in a manner distinct from cyclopamine or side-chain oxysterols. Proceedings of the National Academy of Sciences of the United States of America 113(21).

Traiffort E, Angot E, Ruat M. 2010 Sonic Hedgehog signaling in the mammalian brain. Journal of neurochemistry 113(3):576–590. [PubMed: 20218977]

Van Es S, North KN, McHugh K, De Silva M. 1996 MRI findings in children with neurofibromatosis type 1: a prospective study. Pediatric radiology 26(7):478–487. [PubMed: 8662066]

Halbach O. von Bohlen Und 2010 Dendritic spine abnormalities in mental retardation. Cell and tissue research 342(3):317–323. [PubMed: 21080001]

Wheeler DS, Underhill SM, Stolz DB, Murdoch GH, Thiels E, Romero G, Amara SG. 2015 Amphetamine activates Rho GTPase signaling to mediate dopamine transporter internalization and acute behavioral effects of amphetamine. Proceedings of the national academy of sciences of the United States of America 112(51):E7138–47. doi: 10.1073/pnas.1511670112. Epub 2015 Nov 9. [PubMed: 26553986]

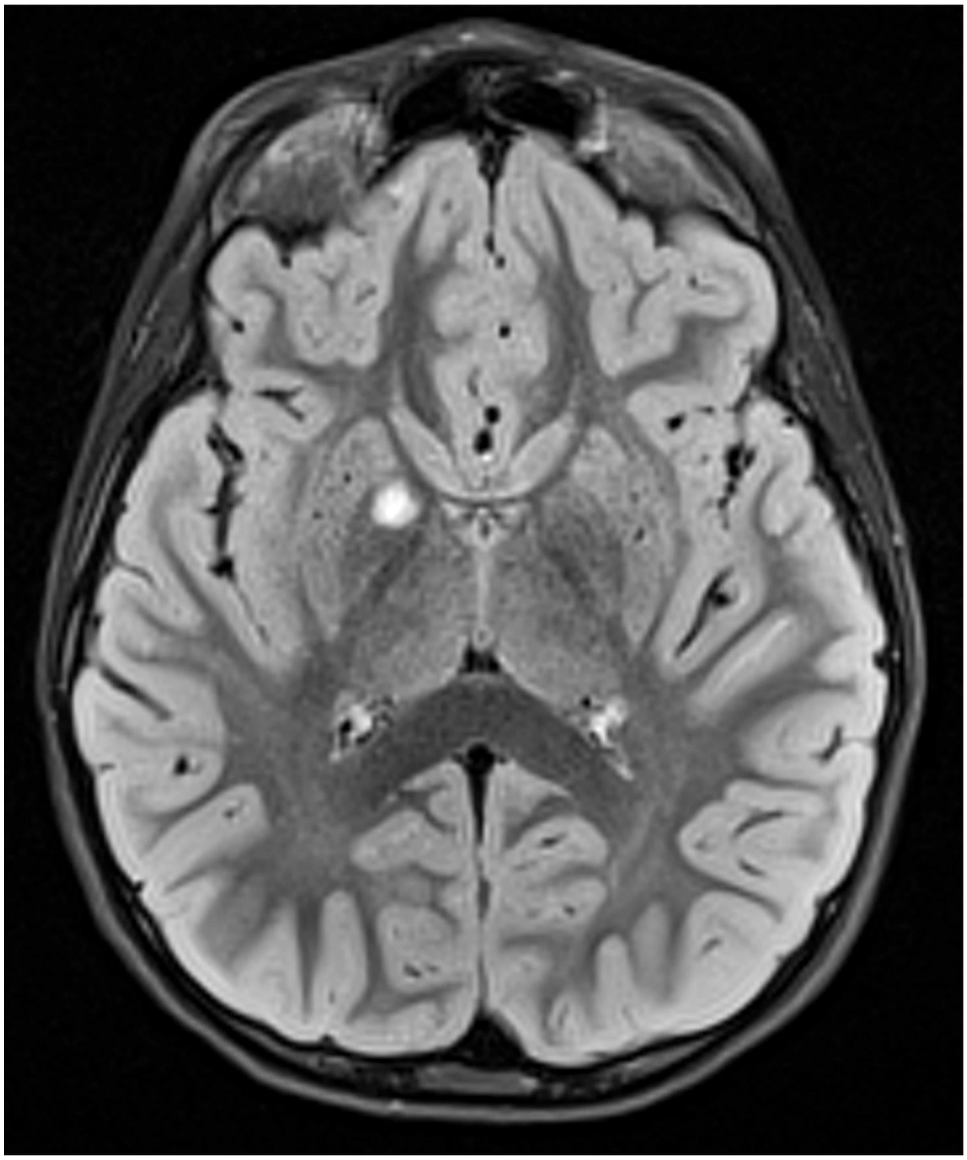

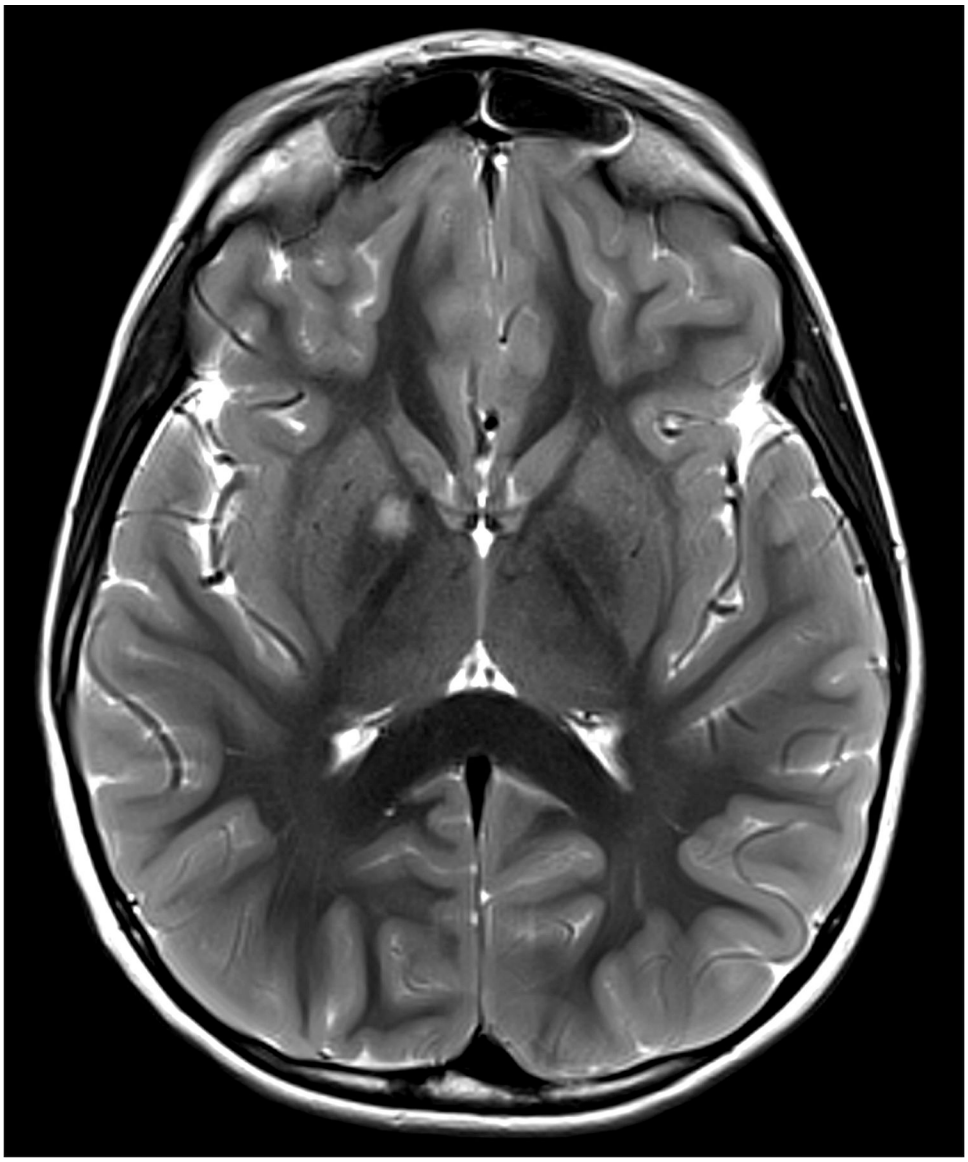

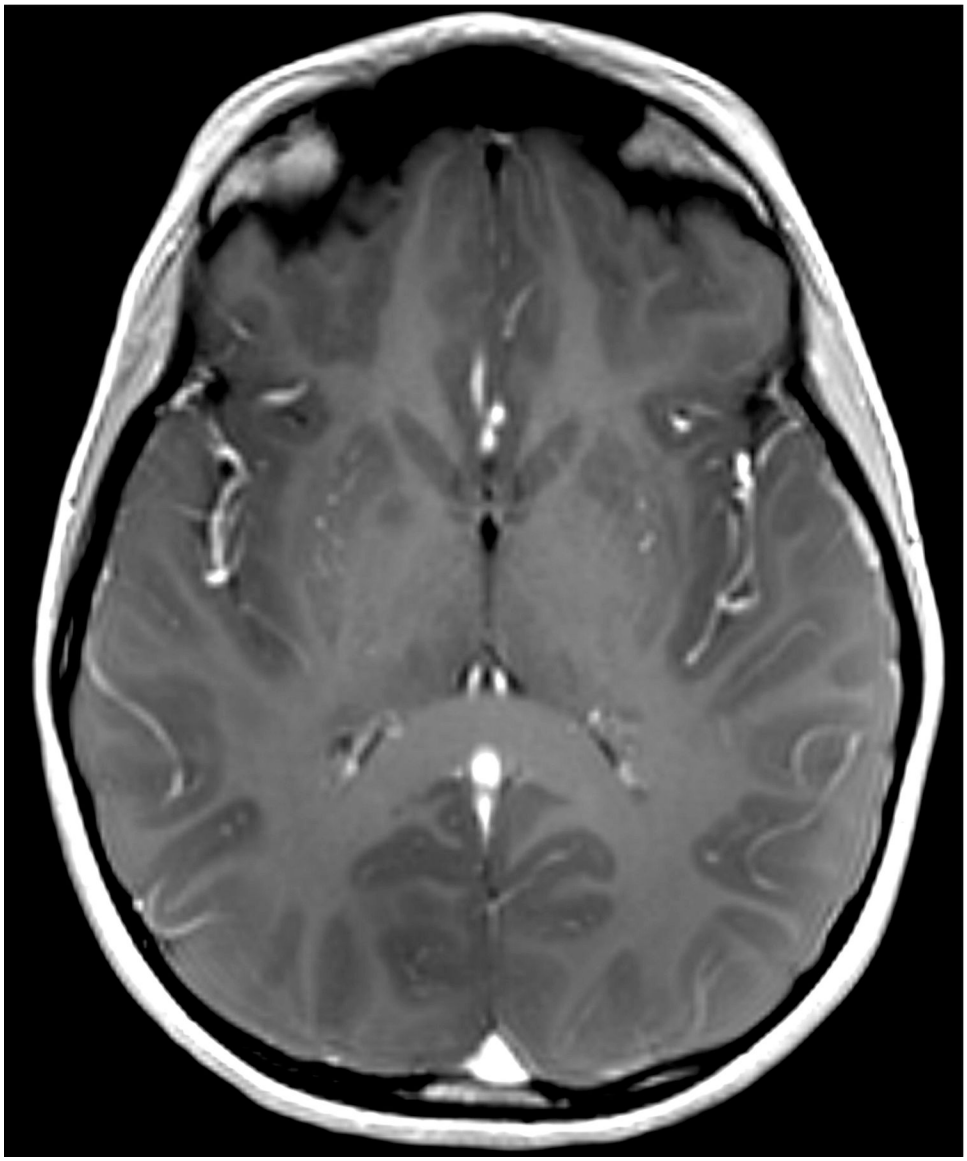

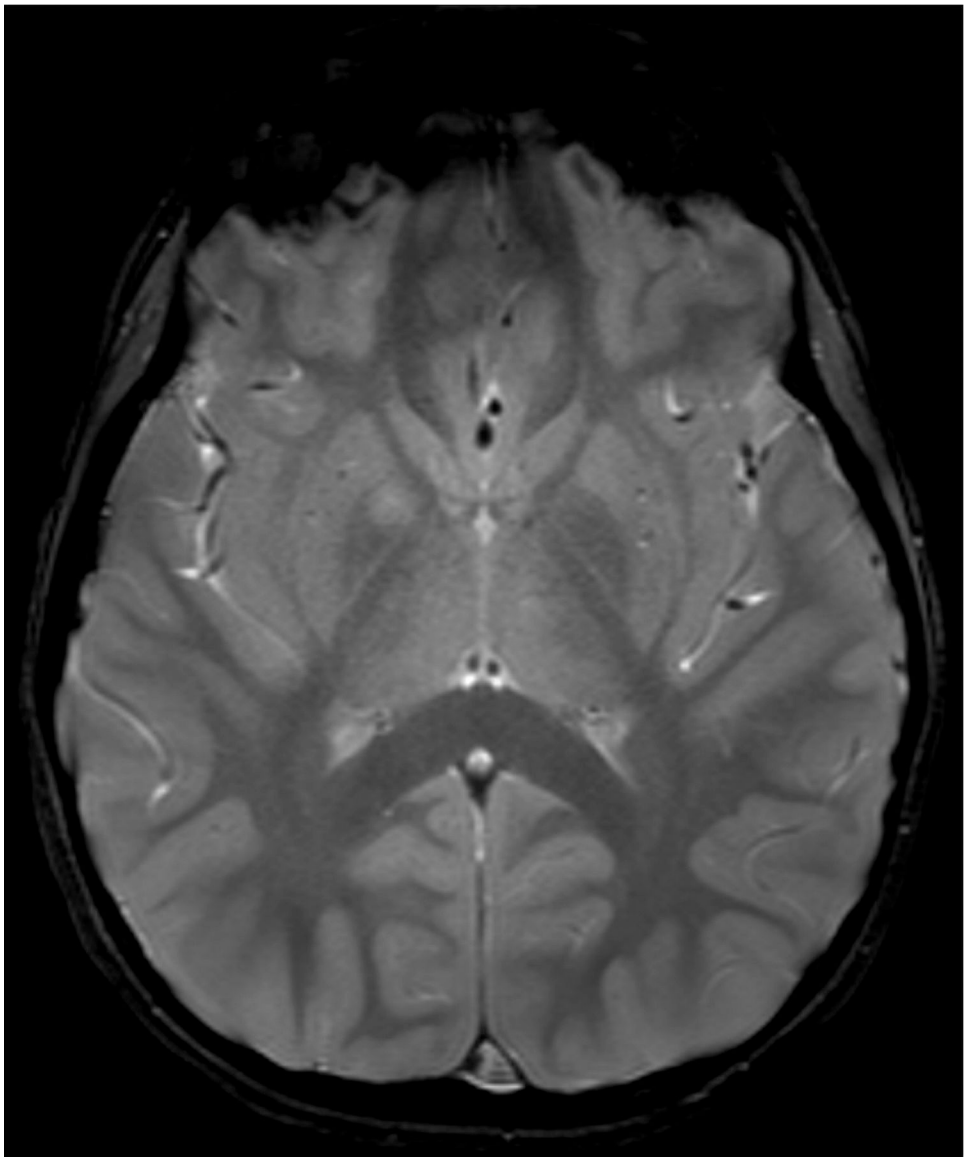

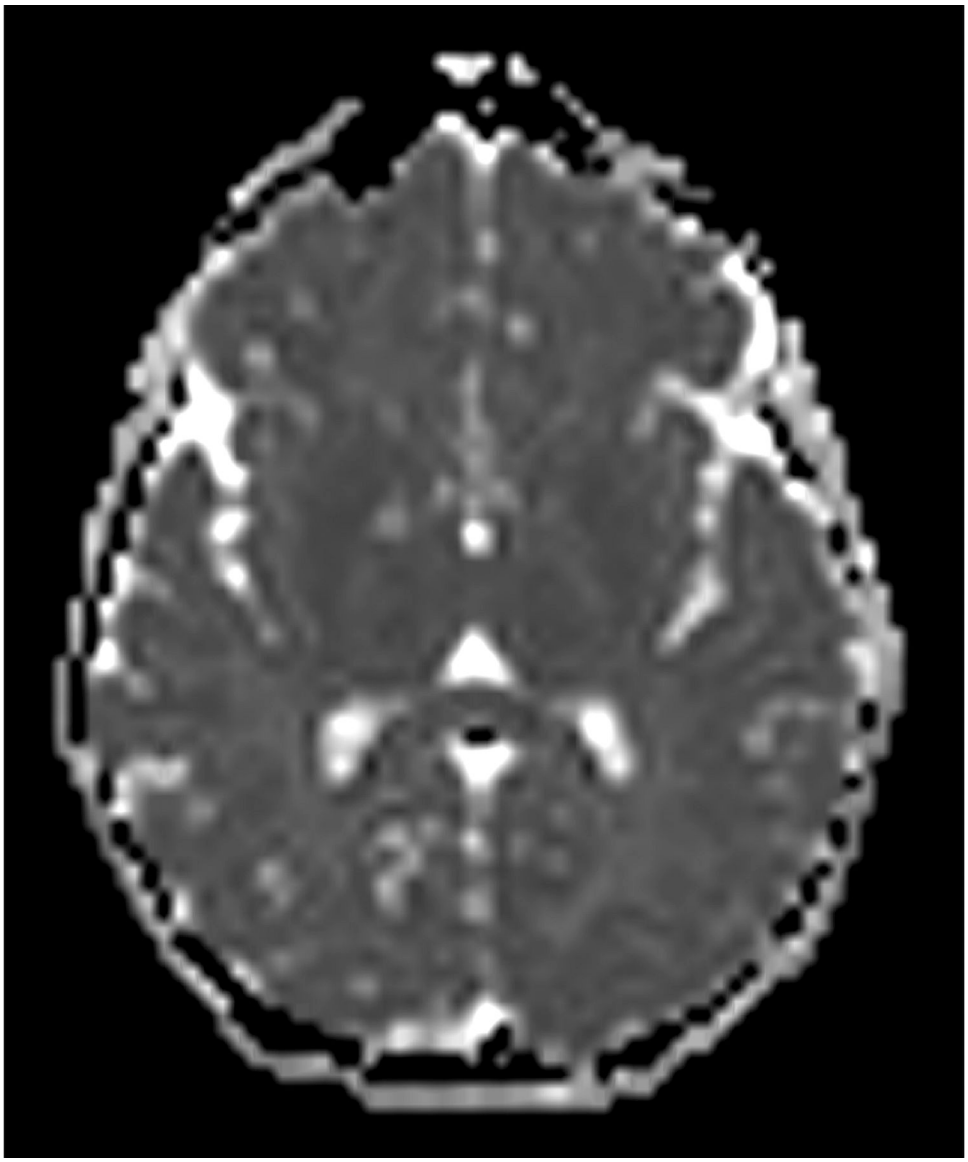

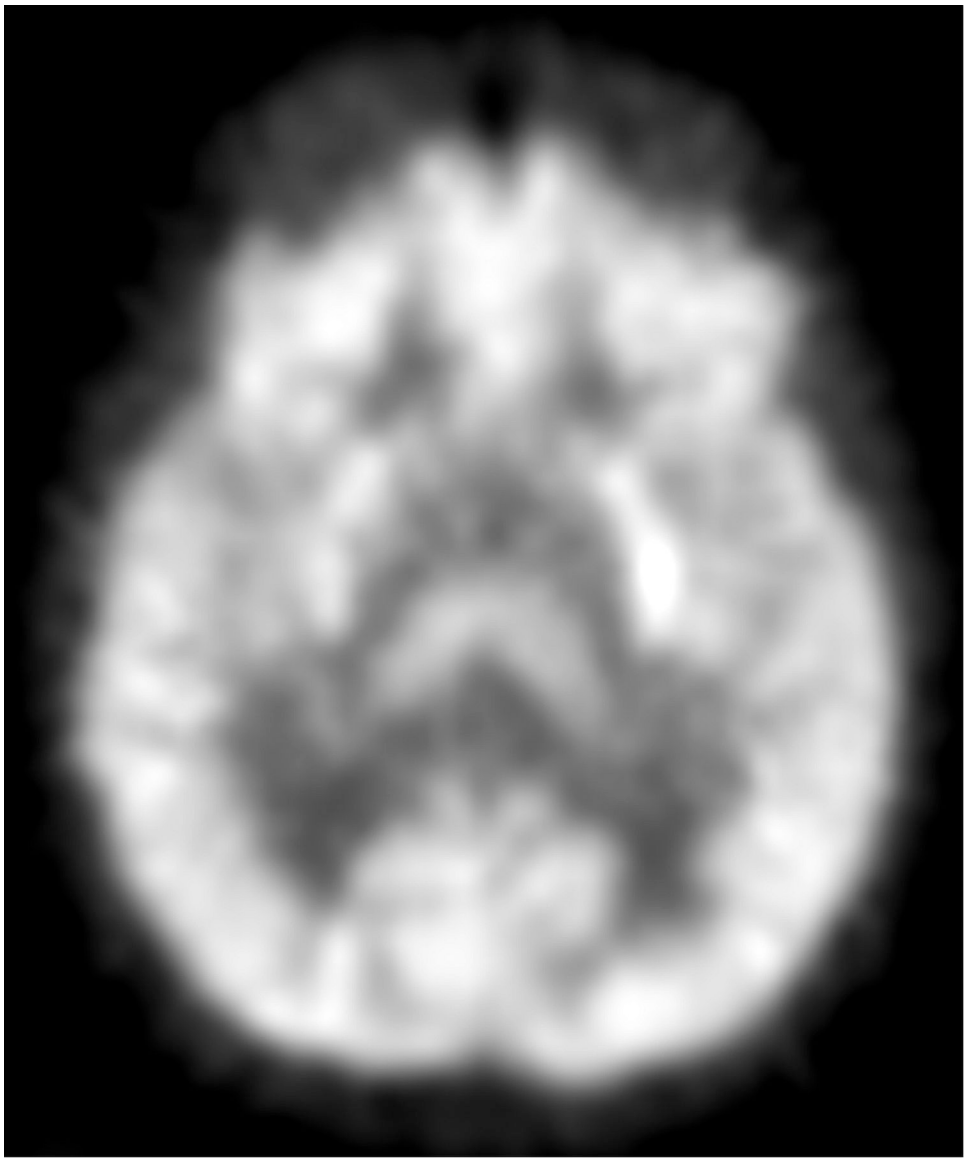

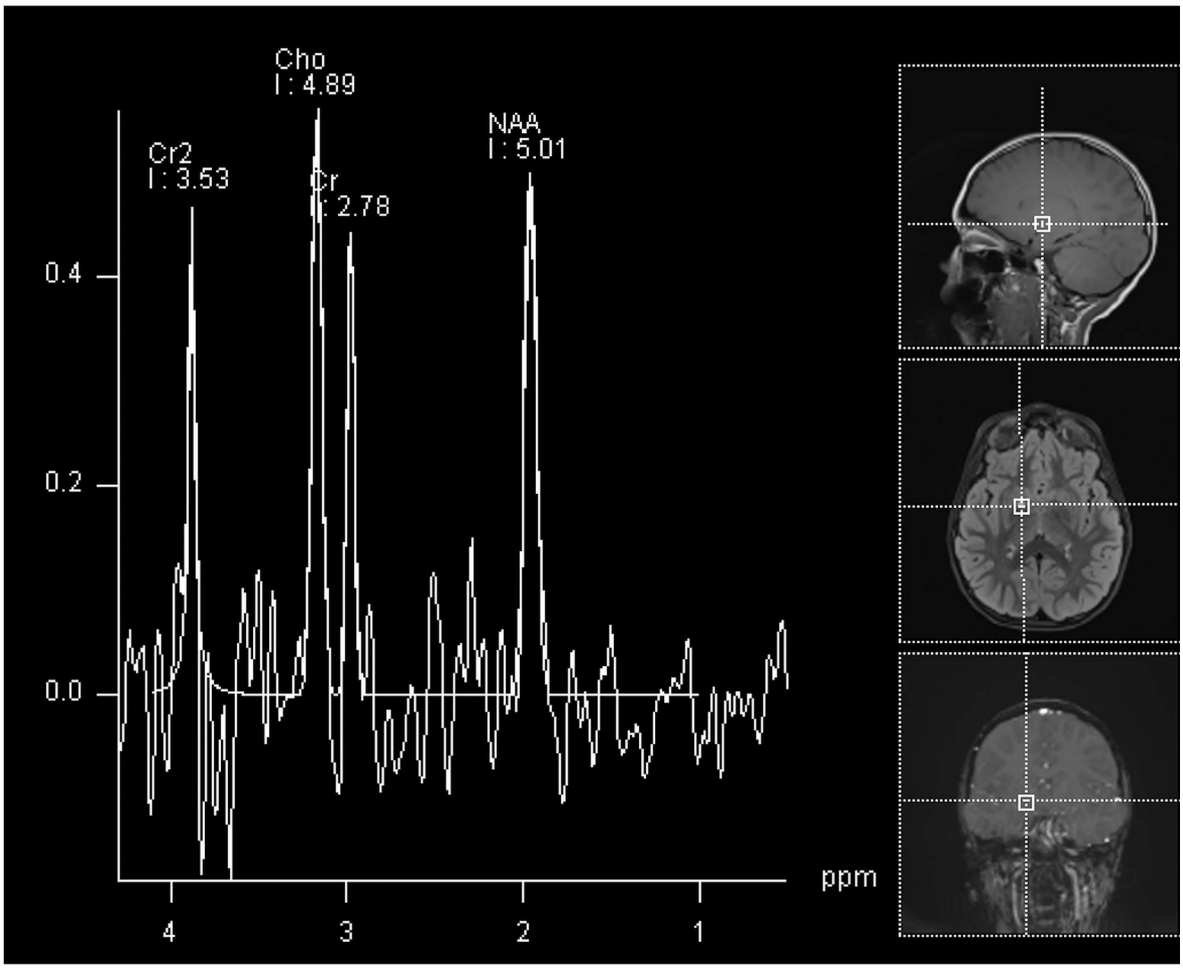

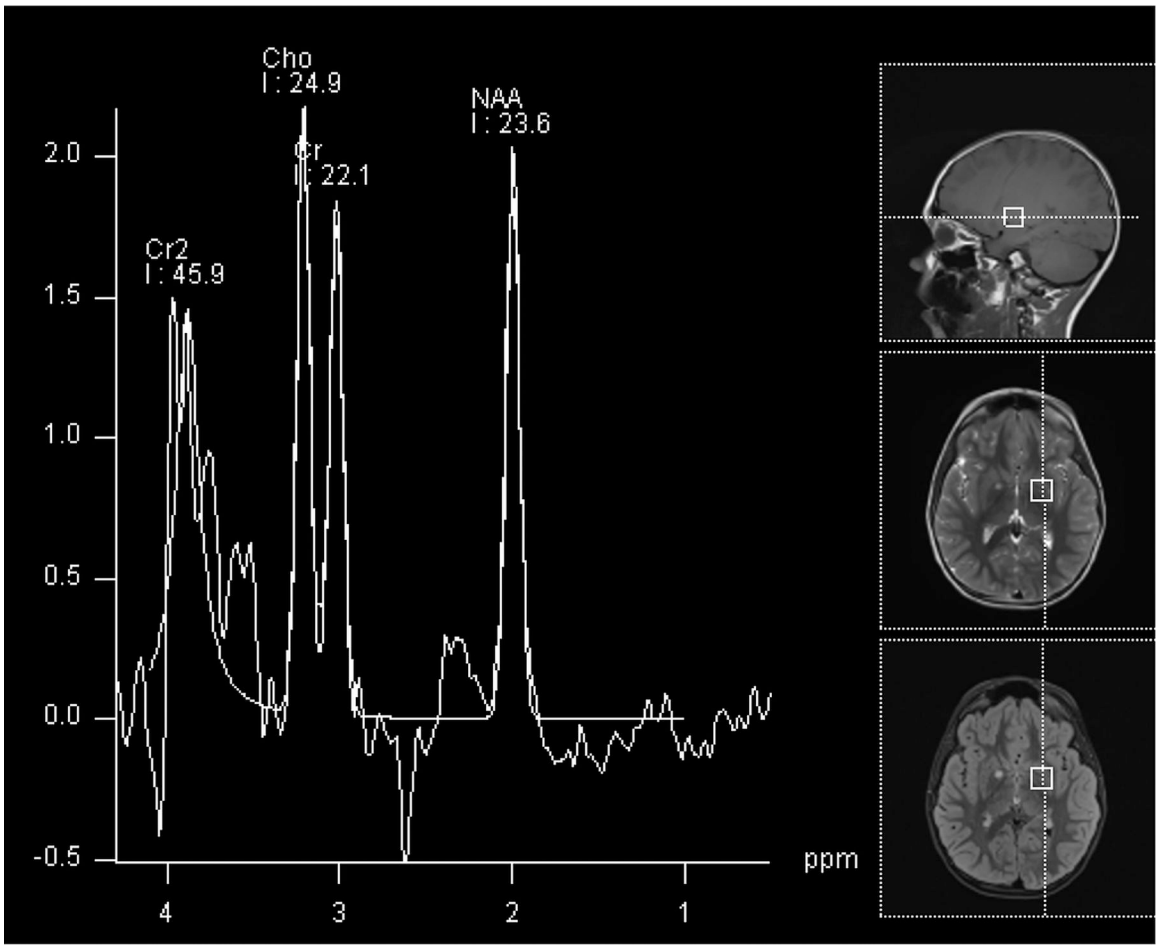

Figure 1.

Imaging characterization of the brain lesions. Except for the location, the imaging characteristics of the lesions were similar for all 3 patients. These images are from Individual 3 at age 8 years 1 month (except for the PET scan, which was obtained at age 7 years 8 months). The FLAIR (A) and T2-weighted (B) images demonstrate a hyperintense lesion with infiltrative qualities in the anterior part of the right globus pallidus. The lesion is hypointense and does not enhance on post-contrast T1-weighted images (C). Susceptibility-weighted images (D) do not demonstrate metal or mineral deposition within the lesion, and the ADC map (E) derived from diffusion tensor imaging (DTI) demonstrates elevated diffusivity within the lesion. FDG-PET(F) demonstrates that tracer uptake within the lesion is indistinguishable from surrounding tissues. A long-echo single voxel ^{1}H MR spectrum (PRESS technique, TE=144 ms, voxel volume = 1 cm^{3}) of the lesion (G) does not differ significantly from a spectrum obtained from the contralateral normal side (H) in the same individual. Maps of relative cerebral blood volume (rCBV), relative cerebral blood flow (rCBF), and relative mean transit time (rMTT) derived from dynamic susceptibility contrast perfusion imaging were unremarkable (images not shown). On all of the imaging sequences, the lesions were homogeneous, without discernable internal structure.

Figure 2.

Temporal evolution of the brain lesions. This is a series of T2-weighted images of Individual 2. At age 3 years 3 months (A) no lesion is visible. At age 4 years 5 months (B), there is a 4 mm lesion in the left anterior pons. At age 5 years 10 months (C), the lesion measures 12 mm and is slightly exophytic. At age 7 years 7 months (D), the lesion remains exophytic and measures its maximum size of 16 mm. At age 16 years 9 months (E), the lesion is no longer visible, but the left anterior pons remains expanded.